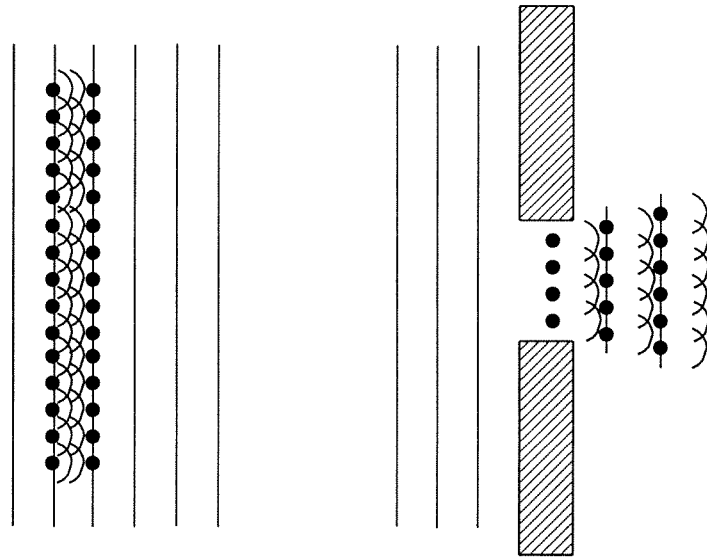


Q1 crib

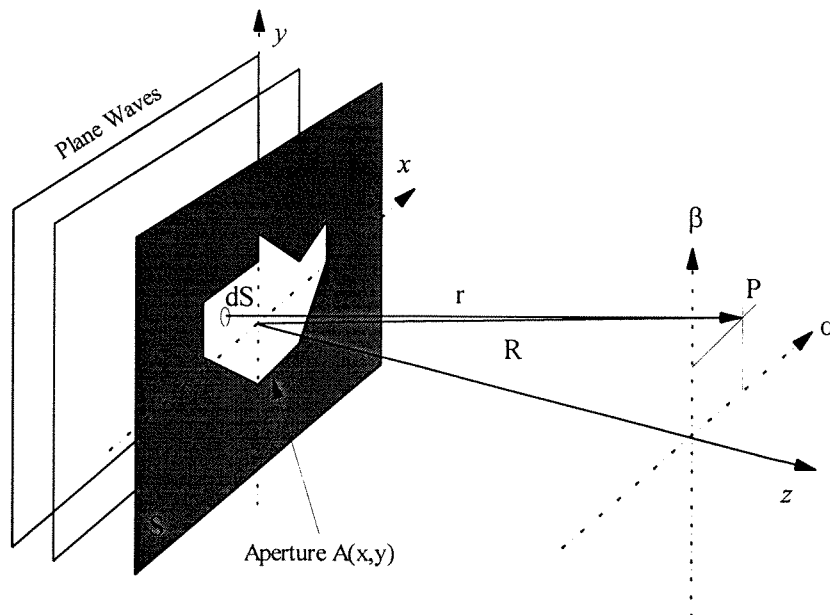
4B11

a) Huygens wavelets can be used to describe and optical propagation in free space. It is the optical equivalent to finite element analysis. The optical field is broken down into an infinite array of point sources. Each wavelet is an ideal point source which appears infinitesimally small in area and radiates perfect spherical wavefronts. Each wavelet propagates spherical wavefronts in all directions, although we only need to consider the wavefronts that are travelling in the same direction as the original optical propagation.



By moving in the direction of propagation, the wavelets can be summed (integrated) at any point to find the optical energy at this new position. This is demonstrated in the diagrams above showing infinite plane wave propagation and the effect of an aperture leading to diffraction.

b)



The total field distribution at P is evaluated by superposition (summation) of all the wavelets across the aperture. The process of interference of these spherical wavelets is

called diffraction and is based on the Huygens-Fresnel approximation. In order to understand and analyse the propagating wavelets, a series of approximations and assumptions must be made. If we consider only the part of the wavelets which are propagating in the forward (+z) direction and are contained in a cone of small angles away from the z axis, then we can evaluate the change in field dE at the point P , due to dS . As the wavelet dS acts as a point source, we can say that the power radiated is proportional to $1/r^2$ (spherical wavefront), hence the field dE will be proportional to $1/r$. We can see that for a real propagating wave of frequency ω and wave number k , ($k = 2\pi/\lambda$) we have the cosine component of a complex wave.

$$dE = \frac{A(x,y)dS}{r} \cos(\omega t - kr)$$

The full complex field radiating from the aperture can be written in terms of exponentials as the cosine is just the real part of the complex exponential.

$$dE = \frac{A(x,y)}{r} e^{j\omega t} e^{-jkr} dS$$

Now, we need to change co-ordinates to the plane containing the point P , which are defined as $[\alpha, \beta]$.

$$R^2 = \alpha^2 + \beta^2 + z^2$$

$$r^2 = (\alpha - x)^2 + (\beta - y)^2 + z^2$$

Which can be rearranged to give.

$$r = R \sqrt{1 - \frac{2\alpha x + 2\beta y}{R^2} + \frac{x^2 + y^2}{R^2}}$$

The final full expression in terms of x and y ($dS = dxdy$) for dE will now be.

$$dE = \frac{A(x,y) e^{j\omega t} e^{-jkR \sqrt{1 - \frac{2\alpha x + 2\beta y}{R^2} + \frac{x^2 + y^2}{R^2}}}{R \sqrt{1 - \frac{2\alpha x + 2\beta y}{R^2} + \frac{x^2 + y^2}{R^2}}} dxdy$$

If the point P is reasonably coaxial (close to the z axis, relative to the distance R) and the aperture $A(x,y)$ is small compared to the distance R , then the lower section of the equation for dE can be assumed to be almost constant and that for all intents and purposes, $r = R$. The similar expression in the exponential term in the top line of the original equation is not so simple. It can not be considered constant as small variations are amplified through the exponential. To simplify this section we must consider only the far field or Fraunhofer region where.

$$R^2 \gg x^2 + y^2$$

In this case, the final term in the exponential ($(x^2 + y^2)/R^2$) can be considered negligible. To further simplify, we use the binomial expansion,

$$\sqrt{(1-d)} = 1 - \frac{d}{2} - \frac{d^2}{8} \dots$$

Hence the simplified version of the field dE , can be expressed as:

$$dE = \frac{A(x, y)}{R} e^{j(\omega t - kr)} e^{jk\left(\frac{\alpha x + \beta y}{R}\right)} dx dy$$

The total effect of the dS wavelets can be integrated across dE to get an expression for the far field or Fraunhofer diffraction pattern.

$$E(\alpha, \beta) = \frac{1}{R} e^{j(\omega t - kR)} \iint_{Aperture} A(x, y) e^{jk(\alpha x + \beta y)/R} dx dy$$

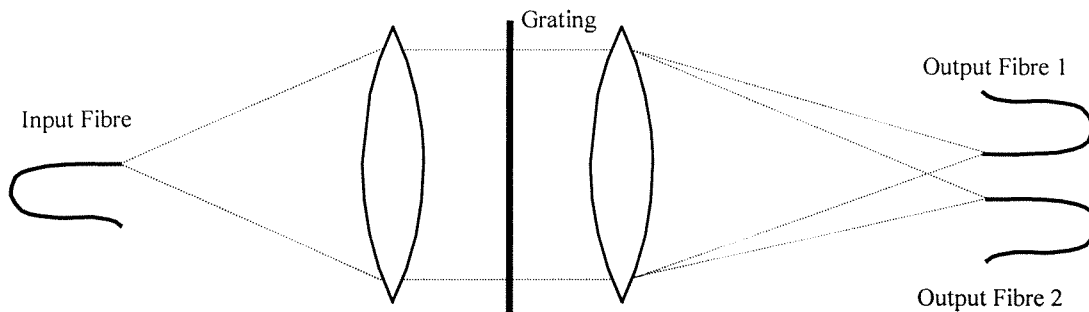
Thus, our final expression for the far field diffraction pattern becomes:

$$E(\alpha, \beta) = \iint_A A(x, y) e^{jk(\alpha x + \beta y)/R} dx dy$$

Hence the far field diffraction pattern at the point P is related to the aperture function $A(x, y)$, by the Fourier transform.

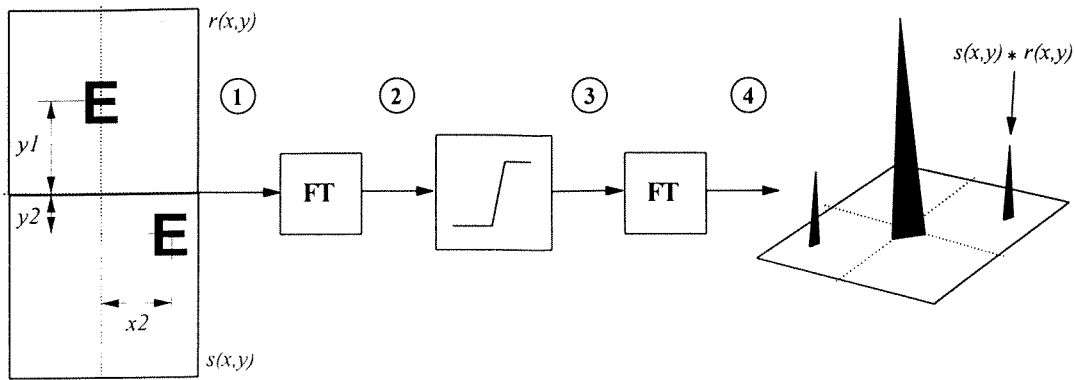
c) The process of diffraction allows us to modify both the spatial and wavelength distribution and of the optical energy passing through the aperture. By changing the shape of the aperture and combining it into arrays of apertures, more complex function such as gratings and holograms can be performed and the light can be steered in terms of both space and wavelength.

The combination of using a lens to perform the Fourier transform and liquid crystal modulators to create a reconfigurable array of apertures allows us to make an optical switch in either space or wavelength. This is usually based around the attractive inverse properties of the 4f optical system.



Q1. Crib

a)



Plane 1 is the input plane with reference and object placed side by side. This is usually done optically using a liquid crystal spatial light modulator.
 Plane 2 is where the joint power spectrum (JPS) is formed via a Fourier transform. This is done optically with coherent illumination and a lens.
 Plane 3 is the non-linearly processed JPS. This can be a simple square law detector like a CCD or CMOS camera and a second LC SLM. Or it can be an optically addressed SLM (OASLM).
 Plane 4 is the output plane formed by another FT lens. This image is usually grabbed by a CCD or CMOS camera.

b) In plane 1, the input $s(x,y)$ and reference $r(x,y)$ are displayed side by side in an optical system and then transformed by a single lens into plane 2.

$$S(u, v)e^{-j2\pi(x_2u - y_2v)} + R(u, v)e^{-j2\pi y_1v}$$

The nonlinearity between planes 2 and 3 creates the correlation and in its simplest form can be modelled by a square law detector such as photodiode or CCD camera which takes the magnitude squared of the light falling upon it.

$$S^2(u, v) + R^2(u, v) + S(u, v)R^*(u, v)e^{-j2\pi(x_2u - (y_1 + y_2)v)} + S^*(u, v)R(u, v)e^{-j2\pi(-x_2u + (y_1 + y_2)v)}$$

The final plane 4 is after the second FT, with the central DC terms proportional to FT $[R^2 + S^2]$ and the two symmetrical correlation peaks spaced by $(x_2, -(y_1 + y_2))$ and $(-x_2, y_1 + y_2)$.

Note, the JTC assumes that the original images are real so that $R(u, v) = R^*(u, v)$ and $S(u, v) = S^*(u, v)$.

c) The JPS of the input now has three components

$$P(u, v)e^{-j2\pi(x_3u - y_3v)} + S(u, v)e^{-j2\pi(x_2u - y_2v)} + R(u, v)e^{-j2\pi y_1v}$$

After the square law non-linearity we now have:

$$\begin{aligned}
& P^2(u, v) + S^2(u, v) + R^2(u, v) + S(u, v)R^*(u, v)e^{-j2\pi(x_2u - (y_1 + y_2)v)} + S^*(u, v)R(u, v)e^{-j2\pi(-x_2u + (y_1 + y_2)v)} \\
& + P(u, v)R^*(u, v)e^{-j2\pi(x_3u - (y_1 + y_3)v)} + P^*(u, v)R(u, v)e^{-j2\pi(-x_3u + (y_1 + y_3)v)} \\
& + S(u, v)P^*(u, v)e^{-j2\pi((x_2 - x_3)u - (y_2 - y_3)v)} + S^*(u, v)P(u, v)e^{-j2\pi(-(x_2 - x_3)u + (y_2 - y_3)v)}
\end{aligned}$$

This plane not only contains the desired RS and RP correlations, it also contains the unwanted cross correlations of P and S which could be as strong or even stronger than the other pairs, leading to incorrect identification of possible correlation peaks.

If P and S match R, then all peaks will be present, hence the extra PS peaks can be eliminated, however if P matches S, then the PS cross correlation will be incorrectly recognised as an SR correlation.

If the unknown input image is displayed and the reference image removed, then the PS correlation will be the only peaks present. If this plane is stored and then R is added to the input, then the PS error peaks can be removed by subtracting the stored plane from the one with R included.

D11 Answers, Question 3

(a) Even over distances of millimetres or less the fixed capacitance associated with an optical interconnection channel can be less than that of an electrical one. The power consumption (energy per bit) is therefore less and the maximum data rate higher. There is no simple way of integrating light sources or modulators into silicon CMOS circuitry. Conventional semiconductor lasers and light emitting diodes cannot be made in silicon because it is a direct bandgap semiconductor.

(b) i. For a remote fanout of F equal tracks the effective electrical track capacitance is increased by a factor F. For an optical interconnection it is the smaller capacitance associated with the photo diode that is multiplied by the factor F. Hence the fanout follows optical interconnections as the gains in power consumption and data rate are enhanced.

ii. Replacing laser sources (such as VCSELs) with optical modulators favors optical interconnections since it avoids the power dissipated in bringing the laser to threshold. The switching energy of a modulator may also be less than the energy to generate photons in a laser.

iii. The effects of decreasing the minimum feature size (a) are complex.

One major influence is that the voltage falls $\left(V \propto 2.9a^{\frac{1}{2}} \right)$

This favors electrical interconnections especially low data rates (in the threshold limited region) where the ratio of the optical to electrical energy per bit

$\left(\frac{E_0}{E_E} \right)$ is proportional to $\frac{1}{2} / 2$

$$\frac{E_0}{E_E} = \frac{2h\nu (C_{pd} + C_{in})}{qV m C_T} + \frac{2\tau P_{th}}{C_T 1/2}$$

Where P_{th} is the laser threshold power, τ is the rise time of the optical interconnection, η is the efficiency of the optical interconnect, and $(C_{pd} + C_{in})$ and C_T are the capacitance's associated with the photodetectors and the electrical interconnect respectively.

A major effect is that (if we ignore fringe fields) the RC time constant associated with an electrical interconnection of a given length remains constant as the feature size (and therefore the conductor width) falls, i.e. there is no increase in signal bandwidth with decreasing geometry. (This contrasts with gate delays and device switching speeds which both decrease markedly.)

iv. The efficiency of a hologram in a free space optical interconnect (e.g. 75%) may well be greater than the launch efficiency into on-chip planar waveguides in guided wave on-chip optical interconnect. Other factors are probably comparable.

- (a) Modulated power of laser $P_L = 1 \text{ MW}$
 Threshold power of laser $P_{th} = 0.5 \text{ MW}$
 Hologram efficiency = 75%
 Laser efficiency = 40%

Therefore;

$$1 = \frac{P}{0.75 \times 0.4} + 0.5$$

Where P = optical power incident on the photodetector measured in milliwatts
 $P = 0.15 \text{ MW}$

- (b) The number of photons incident on the photodetector is therefore

$$\frac{P}{h\nu} \text{ where } h\nu \text{ is the photon energy. Of these } \frac{\eta_D P}{h\nu}$$

are converted to hole-electron pairs so the current generated is

$$I_D = \frac{2qP\eta_D}{h\nu} \text{ Amps where } q \text{ is the electronic charge}$$

Here $h\nu \cong 1 \text{ eV}$ and $q = e$

Therefore $I_D = 2 \times 0.15 \times 0.3 \times 10^{-3} \text{ Amps}$

$$I_D \cong 10^{-4} \text{ A}$$

The maximum data rate D is given by $D = 1/2t$ where t = the rise time of the detector circuit.

$t = 2RC$ where R = the photodetector resistance

C = the total capacitance associated with photodetector (i.e. the photodetector capacitance plus the capacitance of the CMOS gate that it drives, $C_{pd} + C_{in}$)

$$\text{Here } R = \frac{V}{I_D}$$

Where V is the voltage supplied to the photodetector circuit (here 5V)

$$\text{Therefore } R = \frac{5}{10^{-4}} \text{ ohms} = 5 \times 10^4 \text{ ohms}$$

$$\begin{aligned} \text{Therefore } t &= 2 \times 5 \times 10^4 \times 30 \times 10^{-15} \text{ secs} \\ &= 4 \times 10^{-9} \text{ sec} \end{aligned}$$

$$\text{Therefore } D = \frac{1}{2t} = \frac{1}{8 \times 10^{-9}} = 100 \text{ MHz}$$

(d) This maximum data rate could be increased by:

- Increasing the useful laser power i.e. increasing the laser power, or reducing the lasing threshold
- Reducing the capacitance associated with the photodetector

A) The structure & deformations of a nematic liquid crystal are defined in terms of the nematic director \underline{n} which gives the local average orientational order of a large number of rod-like molecules (in dynamic motion).
The basic deformations and their associated elastic constants are

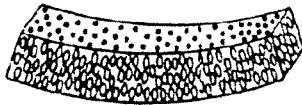
Elastic Constants Defined for Nematic Liquid Crystals

3

Elastic constant

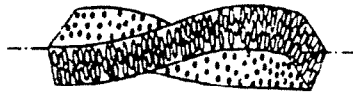
Deformation

Splay --- k_{11}



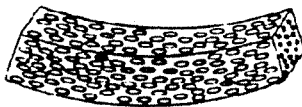
$\nabla \cdot \underline{n}$

Twist --- k_{22}



$\underline{n} \cdot \nabla \times \underline{n}$

Bend --- k_{33}



$\underline{n} \times \nabla \times \underline{n}$

In general:

Stored energy = $\frac{1}{2}$ (some force constant) x (some deformation)

and continuum theory gives the free energy equation

1)

The Volume Density of Free Energy resulting from Elastic Deformations.

The Oseen-Frank Equation.

$$F = \frac{1}{2} k_{11} (\nabla \cdot \underline{n})^2 + \frac{1}{2} k_{22} (\underline{n} \cdot \nabla \times \underline{n})^2 + \frac{1}{2} k_{33} (\underline{n} \times \nabla \times \underline{n})^2$$

splay

twist

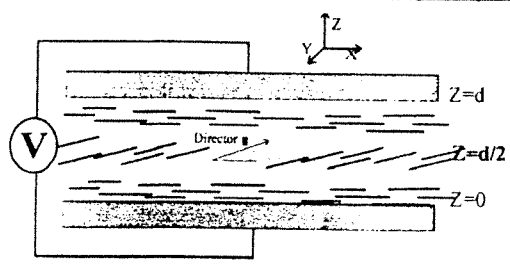
bend

This equation applies to non-chiral-nematic liquid crystals.
It is in Joules per m^3 .

A Fredericksz transition occurs when an external voltage is applied to induce a deformation against a restoring force resulting from surface alignment forces

For small deformations the planar to homeotropic Fredericksz transition depends on the splay elastic constant K_{11}

Fredericksz Transition in a Planar Aligned Nematic Liquid Crystal, S-Mode.



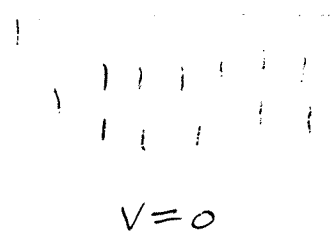
$$E_{\text{threshold}} \cdot d = \pi \left[\frac{k_{11}}{\epsilon_0 \Delta \epsilon} \right]^{1/2}$$

Nematic elastic constants are around 10^{-11} Newtons.
The dielectric permittivity of free space is 8.8 Farads/metre.

**The threshold voltage is independent of thickness d
And is of the order of a few volts.**

To evaluate the twist elastic constant a twisted surface alignment would be used (see below).

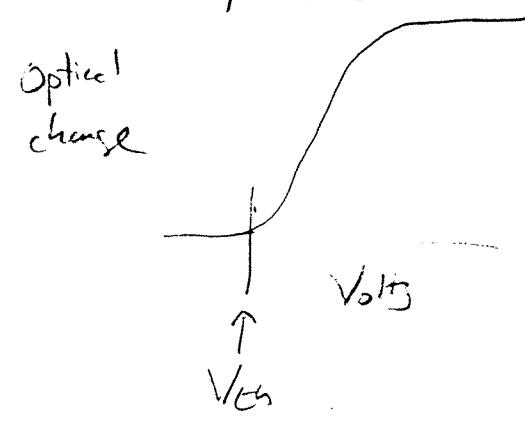
To evaluate the bend elastic constant requires a homeotropic alignment and a transverse electric field



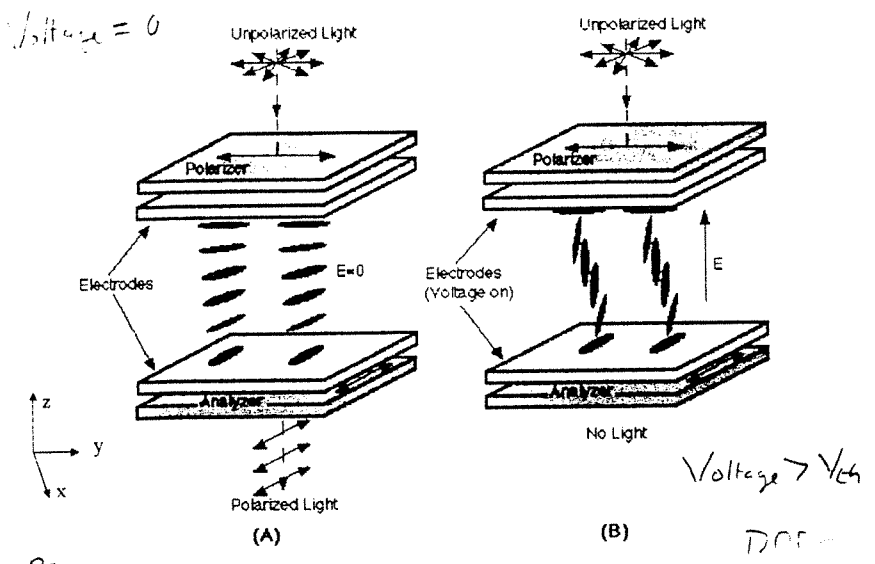
In this case

$$V_{th} = \pi \sqrt{\frac{K_{33}}{\epsilon_0 \Delta \epsilon}}$$

In each case the experimental method is to apply a steadily increasing electric field and measure the onset of an optical change occurring due to the Fredericksz transition, i.e. measure V_{th}



(13)



Principle of Twisted Nematic Display

(2)

The twisted nematic electro-optic effect. Bill Crossland 2001

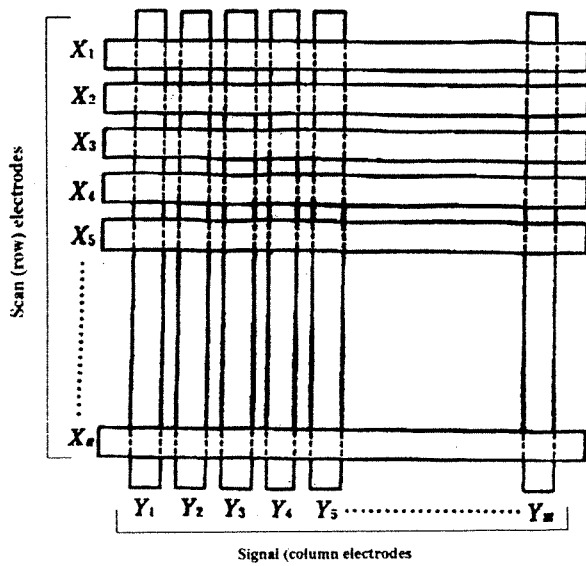
Twisted nematic cells are based on polarisation guiding, down a twisted structure produced by using surface alignment layers and a chiral dopant to ensure a $\pi/4$ twist

For $V > V_{th}$ the twist misaligns and the guiding is lost. Between crossed polarisers this switches from bright to dark

When the field is removed surface alignment forces cause the structure to revert to the original 'OFF' state

(2)

Passive matrix displays have pixels that are addressed via x and y oriented transparent conductors with the pixel being defined by the overlap region

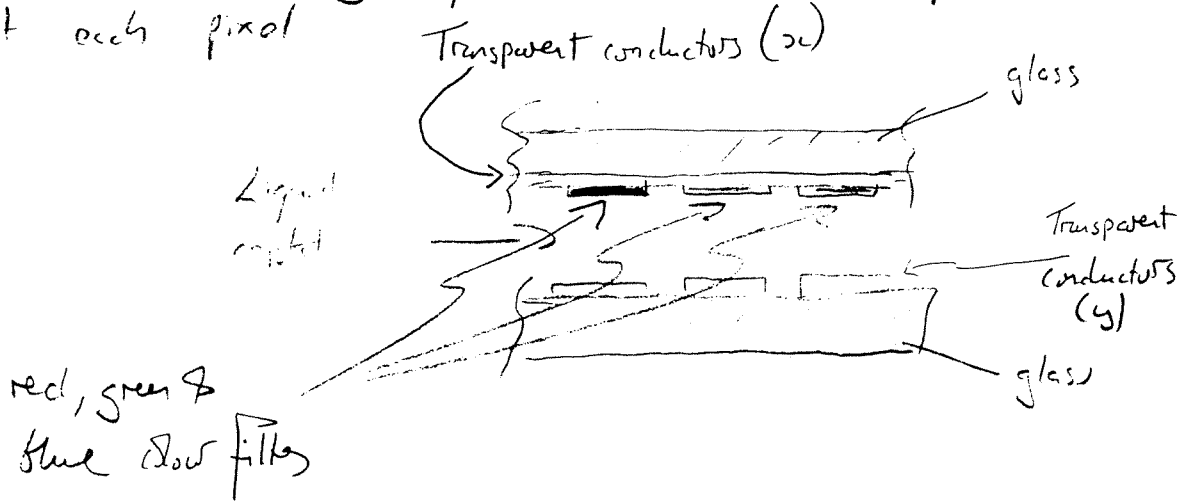


Bill Crossland 2001

Such liquid crystal cells are operated in transmission with a back light

To construct a color display requires red, green or blue filters placed at each pixel

(2)



(C) A planar aligned nematic liquid crystal with a positive dielectric anisotropy undergoes a Fredericksz transition against the splay elastic constant (as illustrated in A)

$$V_{th} = \pi \left[\frac{K_{11}}{\epsilon_0 \Delta \epsilon} \right]^{1/2}$$

$$\therefore K_{11} = \frac{V_{th}^2 \epsilon_0 \Delta \epsilon}{\pi^2}$$

(2)

$$\therefore K_{11} = \frac{1 \times 8.854 \times 10^{-12} \times 8}{\pi^2} \text{ [SI units]}$$

$$\approx 7 \times 10^{-12} \text{ N}$$

(2)